Phytochemistry xxx (2017) 1–8

Contents lists available at ScienceDirect

Phytochemistry

journal homepage: www.elsevier.com/locate/phytochem

Identification and characterization of L-lysine decarboxylase from *Huperzia serrata* and its role in the metabolic pathway of lycopodium alkaloid

Baofu Xu [a, b], Lei Lei [a], Xiaocen Zhu [a], Yiqing Zhou [a], Youli Xiao [a, b, c, *]

[a] CAS Key Laboratory of Synthetic Biology, CAS Center for Excellence in Molecular Plant Sciences, Institute of Plant Physiology and Ecology, Shanghai Institutes for Biological Sciences, Chinese Academy of Sciences, Shanghai, 200032, China
[b] University of Chinese Academy of Sciences, Beijing, 100039, China
[c] CAS-JIC Centre of Excellence in Plant and Microbial Sciences, China

ARTICLE INFO

Article history:
Received 29 September 2016
Received in revised form
23 December 2016
Accepted 29 December 2016
Available online xxx

Keywords:
Huperzia serrata
Lycopodiaceae
Huperzine A
L-lysine decarboxylase
Copper amine oxidase
5-Aminopentanal

ABSTRACT

Lysine decarboxylation is the first biosynthetic step of Huperzine A (HupA). Six cDNAs encoding lysine decarboxylases (LDCs) were cloned from *Huperzia serrata* by degenerate PCR and rapid amplification of cDNA ends (RACE). One HsLDC isoform was functionally characterized as lysine decarboxylase. The HsLDC exhibited greatest catalytic efficiency (k_{cat}/K_m, 2.11 s^{-1} mM^{-1}) toward L-lysine *in vitro* among all reported plant-LDCs. Moreover, transient expression of the HsLDC in tobacco leaves specifically increased cadaverine content from zero to 0.75 mg per gram of dry mass. Additionally, a convenient and reliable method used to detect the two catalytic products was developed. With the novel method, the enzymatic products of HsLDC and HsCAO, namely cadaverine and 5-aminopentanal, respectively, were detected simultaneously both in assay with purified enzymes and in transgenic tobacco leaves. This work not only provides direct evidence of the first two-step in biosynthetic pathway of HupA in *Huperzia serrata* and paves the way for further elucidation of the pathway, but also enables engineering heterologous production of HupA.

1. Introduction

The plant Family Lycopodiaceae comprises major genera *Huperzia (Phlegmariurus), Lycopodium (Diphasiastrum, Lycopodiastrum)* and *Lycopodiella (Palhinhaea)*, with a total of about 500 species worldwide (Zhang et al., 2013; Kitajima and Takayama, 2012; Ma and Gang, 2004). Since Bödeker separated lycopodine, the first structurally characterized lycopodium alkaloid, from *Lycopodium complanatum* in 1881 (Bödeker, 1881), more than 200 lycopodium alkaloids have been identified (Ma and Gang, 2004). The lycopodium alkaloids are quinolizine, pyridine, or α-pyridone type of alkaloids which consist of four structural classes, the lycopodine class, the lycodine class, the fawcettimine class, and the miscellaneous group represented with lycopodine, lycodine, fawcettimine and phlegmarine, respectively (Fig. 1) (Ayer and Trifonov, 1994). With the unique characteristics, the lycopodium alkaloids have shown important biological activities in relation to the cardiovascular or neuromuscular systems and have attracted the attention of many natural product and synthetic chemists (Ma and Gang, 2004; Kitajima and Takayama, 2012). So far, very few biosynthetic studies have been conducted successfully on lycopodium alkaloids (Ziegler and Facchini, 2008; Sun et al., 2012). This lack of knowledge prevents engineering applications for their production through synthetic biology. By contrast, much is known about the biosynthesis of benzylisoquinoline and monoterpene indole alkaloids as well as about glucosinolates (Thodey et al., 2014; Fossati et al., 2015; Brown et al., 2015; Møldrup et al., 2012).

Huperzine A (HupA), one of the pyridine skeleton lycodine, was firstly isolated from the Chinese folk medicinal herb *Qian Ceng Ta* (whole plant of *Huperzia serrata* (*thunb. ex Murray*) *Trev.* (Lycopodiaceae)) in 1986 (Liu et al., 1986a, 1986b). Since HupA was found to possess potent acetylcholinesterase inhibition (AChEI) effect (Tang et al., 1986, 1989) and had been clinically used for the treatment of Alzheimer's disease (AD) for years in China (Bai et al., 2013). On the

* Corresponding author. CAS Key Laboratory of Synthetic Biology, CAS Center for Excellence in Molecular Plant Sciences, Institute of Plant Physiology and Ecology, Shanghai Institutes for Biological Sciences, Chinese Academy of Sciences, Shanghai, 200032, China.
E-mail address: ylxiao@sibs.ac.cn (Y. Xiao).

http://dx.doi.org/10.1016/j.phytochem.2016.12.022
0031-9422/

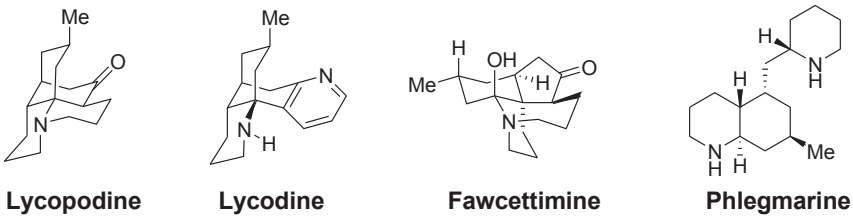

Fig. 1. Representative nature products of the four major classes of Lyocopodium alkaloids.

basis of feeding experiments (Hemscheidt and Spenser, 1993), the first two biosynthetic steps for lycopodium alkaloids are generally believed involving the decarboxylation of lysine to cadaverine followed by the oxidative deamination of cadaverine to 5-aminopentanal (Ma and Gang, 2004) (Fig. 2).

Two enzymes, namely, lysine decarboxylase (LDC) and copper amine oxidase (CAO) function in the HupA biosynthesis pathway have been isolated from *Huperzia serrata* (*H. serrata*) (Bunsupa et al., 2016; Sun et al., 2012). However, LDC from *H. serrata* failed to be purified from recombinant *E. coli* cells (Bunsupa et al., 2016) and lacked direct evidence of its activity. In addition, many other enzymes (P450 etc.) participating in the HupA biosynthesis pathway remain to be identified. What's more, based on the comparison of 454-ESTs studies from *H. serrata,* a unique sequence (GO914645) encoding a full-length LDC-like gene was found, but no biochemical experiment was confirmed the bioactivity so far (Luo et al., 2010).

In this study, six previously undescribed LDCs were isolated from *H. serrata* using degenerate primers based on the conserved sequences of LDC enzymes (Bunsupa et al., 2012) with over 95% nucleotide identify and 98% amino acid identity, and one of them (HsLDC-X1) was functionally characterized in detail. The evidence provided from both *in vitro* and *in vivo* experiments in tobacco (*Nicotiana benthamiana*) suggests that the enzyme identified in this study (HsLDC-X1, which will be referred as HsLDC in the following discussion) functions in decarboxylation of lysine. The enzymatic decarboxylation activities on a variety of amino acids were also evaluated. HsLDC exhibited greater catalytic efficiency to lysine/ornithine than to 7 other selected amino acids. The key residue, K118, for binding of pyridoxal 5'-phosphate (5-PLP) was directly detected by LC-MS/MS consistent with blast analysis. Additionally, with a novel method developed, the enzymatic products of HsLDC and HsCAO, namely cadaverine and 5-aminopentanal, respectively, were detected simultaneously both in assay with purified enzymes and in transgenic tobacco leaves. This research complements the HupA biosynthesis pathway study and paves the way for engineering production of this alkaloid.

2. Results and discussion

2.1. Identification of LDCs from Huperzia serrata

To identify the first gene, L-lysine decarboxylase (LDC), in the biosynthetic pathway of HupA from *H. serrata*, we performed PCR using degenerate primers (Supplemental Table S1) based on conserved amino acid sequences of known lysine decarboxylase genes in NCBI database (Supplemental Table S2) (Bunsupa et al., 2012; Facchini et al., 2000). An inner fragment of 873 bp was initially isolated with degenerate primers by the Reverse Transcription PCR (RT-PCR) method. Nucleotide BLAST search showed that the core fragment shared high similarity with many known complete cDNAs of lysine/ornithine decarboxylases in NCBI database (Supplemental Fig. S1). A full-length cDNA encoding lysine decarboxylase was obtained by 5′- and 3′-RACEs. The obtained full-length sequence was 1530 bp in length, containing a 1407 bp ORF encoding 469 amino acids. An N-terminal PLP binding domain and a C-terminal substrate binding domain were found in the conserve domains analysis and it belongs to type III PLP dependent superfamily enzyme (Supplemental Fig. S2). Six different cDNAs with over 95% identity (based on amino acid sequence) with each other were obtained with a pair of specific primers using high fidelity DNA polymerase (Supplemental Fig. S3 and Sequence Data S1-6). These protein variants may be redundant copies or result from alternative splicing (Hsiao et al., 2016). The diversity of LDC cDNA resources is bound to help promote synthetic biology by supplying abundant genes to be selected to function in a variety of natural products producing hosts, such as *E. coli*, yeast and tobacco etc (Smanski et al., 2016).

Three LDC sequences, BAR42912.1, BAR42913.1 (from *H. serrata*) and BAR42911.1 (from *Lycopodium clavatum*) which have been uploaded onto NCBI database (Bunsupa et al., 2016), are similar to ones we identified (69% identity between HsLDC-X1 and BAR42912.1 or BAR42913.1; 71% identity between HsLDC-X1 and BAR42911.1). The sequence diversity between HsLDCs identified in this study and the ones reported before possibly result from the variant plants drawing from different zones. A phylogenetic tree

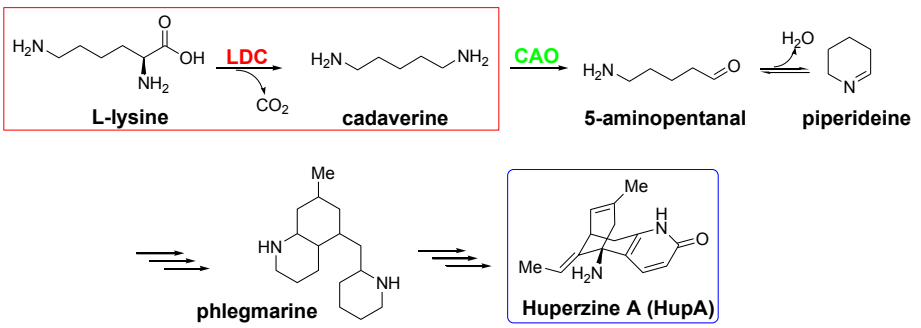

Fig. 2. The proposed biosynthetic pathway of Huperzine A (HupA).

Please cite this article in press as: Xu, B., et al., Identification and characterization of L-lysine decarboxylase from *Huperzia serrata* and its role in the metabolic pathway of lycopodium alkaloid, Phytochemistry (2017), http://dx.doi.org/10.1016/j.phytochem.2016.12.022

was constructed by the Protein Maximum Likelihood method for various plants L/ODCs amino acid sequences. Phylogenetic analysis showed that the plant L/ODCs grouped into three clusters: pteridophytes (red branch), monocots (green branch) and dicots (black branch). HsLDC falls into the clade of pteridophytes and is closely related to other L/ODCs from lycopodium plants suggesting a close evolutionary relationship between them (Fig. 3).

From comparison of 454-ESTs from *H. serrata* analysis, a *LDC*-like gene (GO914645) contained a highly conserved motif PGGXGTXXE was annotated as putative lysine decarboxylase, although evidence for this enzymatic activity was not clear (Luo et al., 2010). Sharing the same highly conserved motif, recombinant His-tagged purified NtMC126 (*MC126* gene from *Nicotiana tabacum*) protein has not exhibited lysine decarboxylase activity in the experiments yet (Häkkinen et al., 2007). This family of *LDC*-like proteins is probably functionally important in the biosynthesis of alkaloids and additional biochemical assays are required to assess its exact function.

2.2. Biochemical characteristics of HsLDC

To determine the biochemical function of HsLDC, the ORF of the gene was cloned into a pET28a expression vector with N-terminal His_6-tag followed by over-expression in *E. coli.* BL21(DE3) cell. HsLDC was purified to near homogeneity with the observed molecular masse of 52.8 kDa on SDS-PAGE in the form of His_6-tag fusion recombinant protein (Fig. 4A, right). The UV-visible absorption spectroscopy of the isolated wide type HsLDC-X1 exhibits the PLP specific peak at 300–350 nm and 410 nm indicating that partial PLP coenzyme incorporated during the protein expression (Coleman et al., 1993; Nishino et al., 1997; Osterman et al., 1999) (Fig. 4B). The PLP binding site of HsLDC can be predicted through seeking for highly conserved amino acid sequence, YAVKCN. PLP is believed to be anchoring at the 'K' residue site through Schiff base linkage between aldehyde group of PLP and ε-amino group of this lysine residue. To identify the key lysine residue, we performed LC-MS/MS analysis of tryptic digests of the $NaBH_4$-reduced the as-isolated HsLDC protein (Ishii et al., 1996). The K118 was identified as the PLP binding residue with the increase of 231.02966 Da which was consistent with the PLP modification at the peptide (Fig. 4C and Supplemental Table S3). In addition, the significance of K118 residue was evaluated through site-directed mutation of the conserved K to A. The HsLDC-K118A mutant was constructed (Supplemental Table S1) and successfully purified to near homogeneity (Fig. 4A, left). By contrast, absorbance intensities at 300–350 nm and 410 nm in the UV-Vis absorption spectra of the K118A mutant were not prominent, suggesting the PLP binding activity was severely affected (Fig. 4B).

With the holoprotein HsLDC harboring PLP cofactor in hand, the decarboxylation activities toward 9 selected amino acid substrates were monitored in the presence of the purified HsLDC and excess amount of PLP using PEPC (PEP Carboxylase) and MDH (Malate Dehydrogenase) coupling assay method (Osterman et al., 1994) (Supplemental Method S1). The decarboxylation activities of purified HsLDC toward the 9 amino acids were evaluated and the detailed kinetic parameters were listed (Table 1). Both L-lysine and L-ornithine were HsLDC optimum substrates, with a k_{cat} of 1.85 s^{-1}

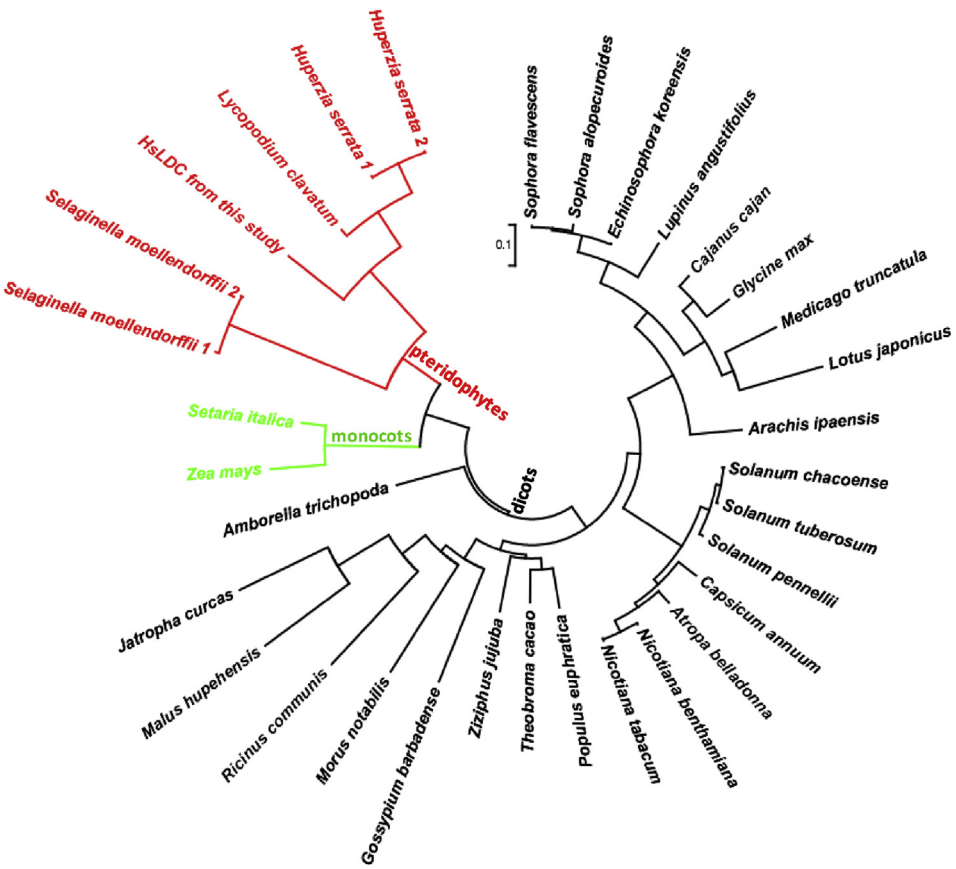

Fig. 3. Phylogenetic tree of L/ODCs proteins from various plant species. Unrooted protein maximum likelihood Phylogenetic tree of selected L/ODC were constructed. Evolutionary analyses were conducted in MEGA6. Analysis showed that the plant L/ODCs grouped into three clusters: pteridophytes (red branch), monocots (green branch) and dicots (black branch). The indicated scale represents 0.1 amino acid substitutions per site. (For interpretation of the references to colour in this figure legend, the reader is referred to the web version of this article.)

Please cite this article in press as: Xu, B., et al., Identification and characterization of L-lysine decarboxylase from *Huperzia serrata* and its role in the metabolic pathway of lycopodium alkaloid, Phytochemistry (2017), http://dx.doi.org/10.1016/j.phytochem.2016.12.022

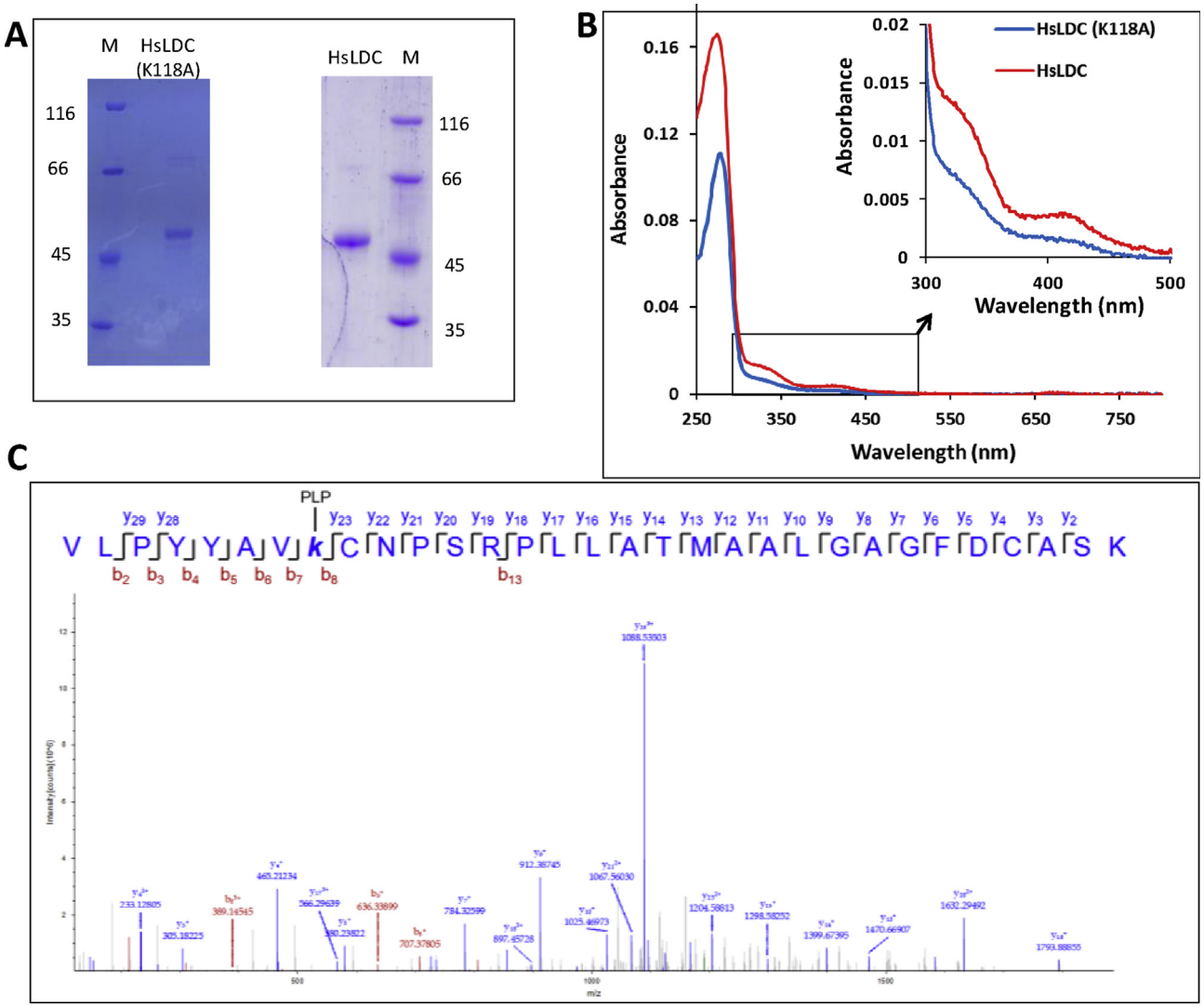

Fig. 4. Biochemical characterization of HsLDC and HsLDC-K118A. (A) SDS-PAGE analysis of purified of HsLDC (right) and HsLDC-K118A (left). (B) UV-visible absorption spectroscopy of 34 μM of HsLDC (Red line) and 34 μM of HsLDC-K118A (Blue line). Insert is the enlarged spectra in the scale of 300–500 nm. (C) LC-MS/MS analysis of tryptic digests of the $NaBH_4$-reduced HsLDC. K118 was identified as the conserved L-Lys residue anchored by PLP. (For interpretation of the references to colour in this figure legend, the reader is referred to the web version of this article.)

Table 1
Kinetic parameters of HsLDC towards 9 selected amino acids.

Entry	Substrate	K_m (mM)	k_{cat} (s^{-1})	k_{cat}/K_m (s^{-1} mM^{-1})
1	L-lysine	0.878 ± 0.0271	1.85 ± 0.0292	**2.11 ± 0.0994**
2	L-ornithine	1.43 ± 0.0442	2.78 ± 0.0431	**1.94 ± 0.0912**
3	D-lysine	1.64 ± 0.0503	0.102 ± 0.00201	0.0625 ± 0.00324
4	L-arginine	0.209 ± 0.00623	0.0859 ± 0.00134	0.412 ± 0.0193
5	L-cysteine	1.32 ± 0.0401	0.155 ± 0.00212	0.117 ± 0.00635
6	L-methionine	0.194 ± 0.00616	0.0859 ± 0.00125	0.442 ± 0.0211
7	L-norleucine	1.07 ± 0.0332	0.102 ± 0.00243	0.0957 ± 0.00514
8	L-valine	5.77 ± 0.0176	0.214 ± 0.00312	0.0371 ± 0.00234
9	L-phenylalanine	15.7 ± 0.479	0.404 ± 0.00632	0.0257 ± 0.00136

Kinetic parameters were calculated from mean values of measurements (n = 3).
Bold represents the greatest activity in the reported plant-LDCs.

and a K_m of 0.878 mM for L-lysine and a k_{cat} of 2.78 s^{-1} and a K_m of 1.43 mM for L-ornithine, respectively (Table 1, entries 1 and 2). The specificity constant k_{cat}/K_m for L-lysine (2.11 s^{-1} mM^{-1}) was slightly greater than for L-ornithine (1.94 s^{-1} mM^{-1}) and both of which were greater than the reported plant-LDCs (Supplemental Table S4) (Bunsupa et al., 2012, 2016). The HsLDC showed more than 30-fold greater catalytic efficiency (k_{cat}/K_m) to L-lysine than to D-lysine (Table 1, entries 1 and 3) which suggested the indispensable significance of the configuration of amino group of HsLDC substrate. In addition, HsLDC showed greater catalytic efficiency to amino acid

Please cite this article in press as: Xu, B., et al., Identification and characterization of L-lysine decarboxylase from *Huperzia serrata* and its role in the metabolic pathway of lycopodium alkaloid, Phytochemistry (2017), http://dx.doi.org/10.1016/j.phytochem.2016.12.022

substrates with N or S heteroatom in the R group than to the aliphatic amino acids with only one amino group or aromatic amino acids (Table 1, entries 4–6 vs 7–9). The decarboxylation activity of L-lysine catalyzed by HsLDC-K118A was evaluated using a derivatization assay (Phan et al., 1982). Comparing to the HsLDC, the activity of HsLDC-K118A towards L-lysine severely decreased about 90% (Supplemental Fig. S14).

2.3. The in vitro preparation of 5-aminopentanal with the HsLDC-CAO coupled assay

L-lysine was incubated with HsLDC in the presence of PLP, the product cadaverine was detected directly by LC-MS (Supplemental Fig. S5). Cadaverine could also be derived quantitatively by reacting with 3, 5-dinitrobenzoyl chloride (Fig. 5A) (Pinto et al., 2014). The benzoylation product, designated as **derivative A**, was fully characterized by MS, ^{1}H-NMR and ^{13}C-NMR and confirmed with the chemical synthesized standard (Fig. 5B and C; Supplemental Figs. S6–S9; Supplemental Method S2).

HsCAO recombinant protein was also successfully purified and characterized as the previous HsCAO report (Supplemental Fig. S10) (Sun et al., 2012). 5-Aminopentanal in the second committed step catalyzed by CAO could be also derived to the benzoylation product, designated as **derivative B**, with the treatment of $NaBH_4$ and then of 3, 5-dinitrobenzoyl chloride (Fig. 5D and E). The 5-aminopentanol group was clearly detected in the **derivative B** from the structural chemical analysis and confirmed by chemical synthesized standard (Supplemental Figs. S11–S12; Supplemental Method S3). With two enzymes, HsLDC and HsCAO, in hand and the novel detection method developed, the HsLDC-CAO coupling assay was performed in one-pot reaction (Fig. 5A; Supplemental Method S4). The intermediate, cadaverine, and the final specialised product, 5-aminopentanal, were monitored by HPLC and confirmed by LC-MS in the form of **derivative A** and **derivative B** after derivatization (Fig. 5A, D and E). Though the catalytic efficiency of HsLDC was slightly less than HsCAO (k_{cat}/K_m, 3.3 s^{-1} mM^{-1}) *in vitro*, the one-pot reaction catalyzed by HsLDC and HsCAO in the same concentration were still necked by the second step with accumulation of more cadaverine than 5-aminopentanal (Fig. 5D). This may be due to differential cofactors interaction and redox environment between the *in vitro* and *in vivo* condition.

2.4. Verification of HsLDC activity and synthesis of 5-aminopentanal in vivo (tobacco leaves)

To confirm whether HsLDC functions *in vivo*, Agrobacterium

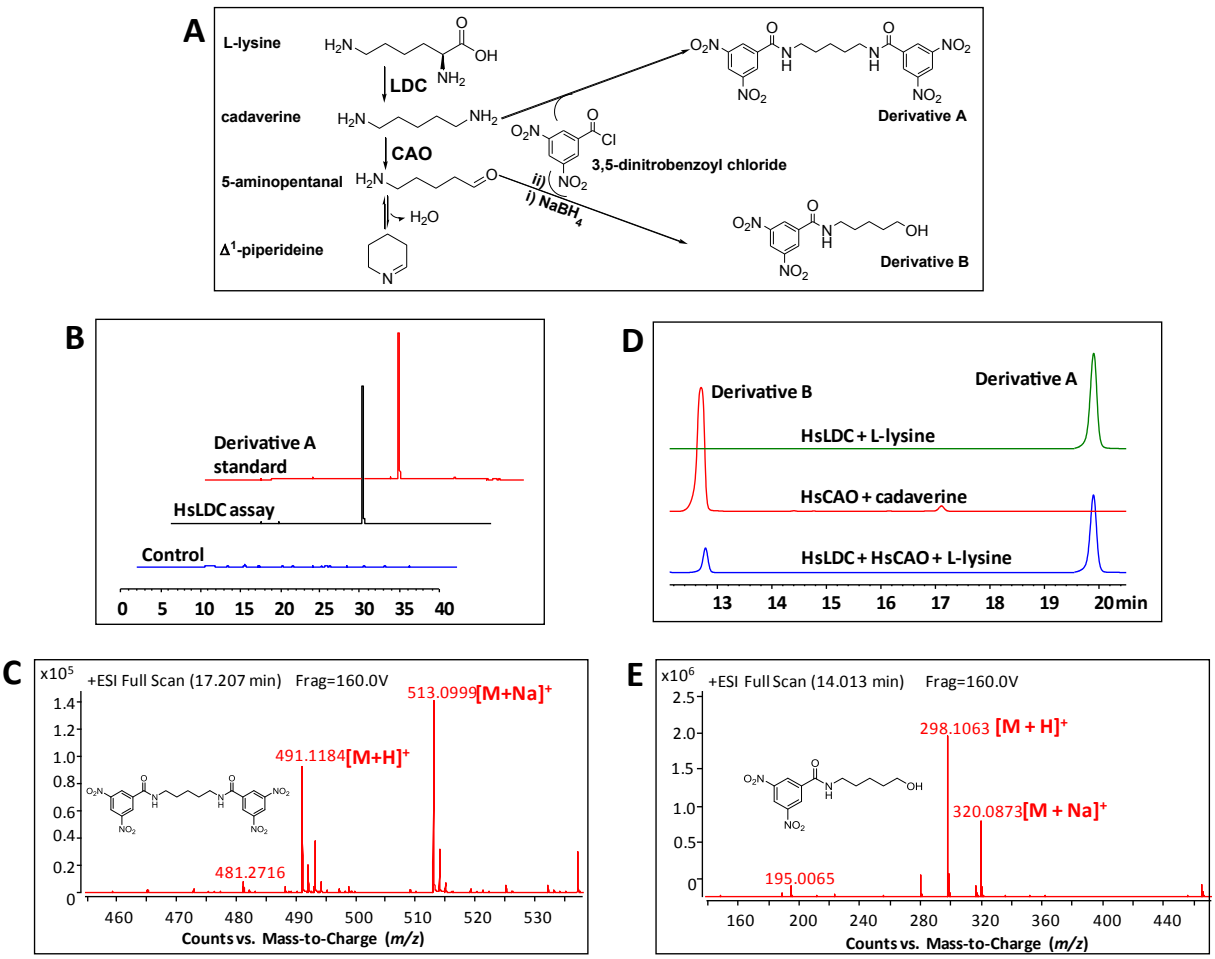

Fig. 5. Chemo-enzymatic *In vitro* assays catalyzed by HsLDC or/and HsCAO. (A) Derivatization method for simultaneously monitoring specialised products catalyzed by LDC and CAO. (B) HPLC analyses of the *in vitro* reactions of the HsLDC after derivatization (from bottom to top, control without L-lysine, full assay, chemical synthesized **derivative A** standard). (C) The MS spectrum of the **derivative A** produced from the derivative enzymatic assay. (*m/z* 491.1184 $[M+H]^+$, $C_{19}H_{19}N_6O_{10}$, calcd for 491.1163; *m/z* 513.0999 $[M+Na]^+$, $C_{19}H_{18}N_6O_{10}Na$, calcd for 513.0982). (D) HPLC analyses of the *in vitro* two enzymes one-pot reactions after derivatization (from top to bottom: the L-lysine as substrate catalyzed by HsLDC, the cadaverine as substrate catalyzed by HsCAO, the L-lysine as substrate catalyzed by HsLDC-CAO). (E) The MS spectrum of the **derivative B** produced from the derivative enzymatic assay catalyzed by HsCAO. (*m/z* 298.1063 $[M+H]^+$, $C_{12}H_{16}N_3O_6$, calcd for 298.1039; *m/z* 320.0873 $[M+Na]^+$, $C_{12}H_{15}N_3NaO_6$, calcd for 320.0859).

Please cite this article in press as: Xu, B., et al., Identification and characterization of L-lysine decarboxylase from *Huperzia serrata* and its role in the metabolic pathway of lycopodium alkaloid, Phytochemistry (2017), http://dx.doi.org/10.1016/j.phytochem.2016.12.022

suspensions, which contained HsLDC expressing vector harboring 35S promoter, were infiltrated into the underside of *N. benthamiana* leaves. RT-PCR analysis confirmed the expression of HsLDC in all HsLDC transformed leaves (Supplemental Fig. S13). Then the content of cadaverine was analyzed in tobacco leaves with the detection method we developed. Comparing with the standard in the HPLC trace, there was no detectable **derivative A** (cadaverine derivative) signal in the wild-type and blank vector transformed tobacco leaves (Fig. 6; Fig. 7, trace e and f; Supplemental Fig. S14A). For the HsLDC transformed leaves, a new peak at t_R = 29.5 min, which was consistent with the **derivative A** was detected with the content 0.75 mg g^{-1} of dry mass which was two orders of magnitude greater than the reported plant derived LDC in plant system (Fig. 6; Fig. 7 trace c; Supplemental Fig. S14A; Supplemental Tables S5–7). By contrast, the HsLDC transgenic tobacco leaves contained a similar level of putrescine (about 20% content of cadaverine), the decarboxylation product of L-ornithine, to the control ones (Supplemental Table S6). To our knowledge, the 5-fold greater content of cadaverine than putrescine in the plant derived LDC transgenic plants was firstly observed. The *in vivo* result indicated that HsLDC was more specific to L-lysine than to L-ornithine which was different from results *in vitro* above and reported before (Bunsupa et al., 2012, 2016).

When the HsCAO was co-transformed with HsLDC into the tobacco leaves, the content of **derivative A** decreased dramatically about 90% (Fig. 6; Fig. 7, trace d; Supplemental Fig. S14 A) and a new peak at t_R = 16.5 min consistent with **derivative B** was detected from the extracts compared with wild-type and blank vector transformed tobacco leaves (Fig. 7, trace d, e and f), which indicated HsCAO was more functional than HsLDC *in vivo,* which was contrary to the one-pot reaction of *in vitro* assay. This result suggested that the HsLDC may function as a rate-limited step in the biosynthesis of lysine-derived alkaloids in plant.

3. Conclusions

The results in this study not only provides direct evidence of the first two-step in biosynthetic pathways of the lycopodium alkaloids and paves the way for further elucidation of the pathway, but also enables engineering heterologous production of the bioactive lycopodium alkaloids, like HupA, lycopodine, and fawcettimine in model hosts. High demand of HupA in the market leads to plants of *H. serrata* continue to be harvested from the wild and causes rapid loss of the resource. Moreover, *H. serrata* plants grow very slowly and are only found in very specialised regions (Ma et al., 2006). Study of HupA biosynthesis genes may help construction of engineered hosts to produce HupA industrially in the future. (Facchini and De Luca, 2008; Thodey et al., 2014; Fossati et al., 2015; Brown et al., 2015).

In preparation of the manuscript, a bifunctional decarboxylase LcL/ODC from *Lycopodium clavatum* which didn't produce HupA based on the author's detection was reported (Bunsupa et al., 2016). The LcL/ODC exhibits slightly less activity than HsLDC-X1 with k_{cat}/K_m of 1.88 s^{-1} mM^{-1} to 2.11 s^{-1} mM^{-1} over L-lys, respectively (Supplemental Table S4). In addition, there was more putrescine produced over cadaverine in the LcL/ODC transgenic Arabidopsis which is contrary to our study (Supplemental Table S7). Even though two cDNA sequences encoding LDCs were identified from *H. serrata* in the report (Bunsupa et al., 2016), due to the insoluble issue, there was no biochemical characterization either *in vitro* or *in vivo* towards the decarboxylation activity on L-lysine or L-ornithine of which we both did successfully.

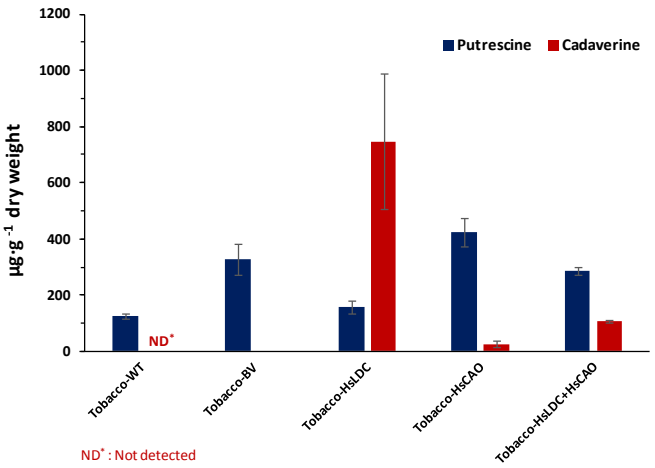

Fig. 6. Quantification analyses of cadaverine and putrescine in transgenic tobacco leaves. The contents of cadaverine and putrescine in transgenic tobacco leaves expressing HsLDC and/or HsCAO. Each bar represents the mean ± SD of three biological replicates for each independent line. BV represents tobacco leaves transformed with blank vector. HsLDC represents tobacco leaves expressing L-lysine decarboxylase (cloned and identified in this study) from *H. serrata*. HsCAO represents tobacco leaves expressing copper amine oxidase from *H. serrata*.

4. Experimental

4.1. Plant materials

Huperzia serrata (*thunb. ex Murray*) *Trev.* (Lycopodiaceae) whole plants were collected from Yongshun, Xiangxi, Hunan, China. After whole plants were transported to our laboratory, they were carefully rinsed in running tap water and soil was removed by hand. Part of young leaves, stem and root were collected separately and immediately frozen in liquid nitrogen, then stored at −80 °C.

4.2. mRNA Extraction and cDNA template preparation

Total RNA from *H. serrata* young leaves was extracted using plant RNA prep pure Plant Kit following the manufacturer's instructions (TIANGEN). RNA quantity, purity and integrity were verified by electrophoresis on 1% agarose gel and NanoDrop Spectrophotometer (Thermo Scientific). The cDNA was synthesized using the Reverse Transcriptase M-MLV (TaKaRa) and Oligo (dT) primers.

4.3. Clone of cDNAs encoding LDC from H. serrata

Degenerate primers were designed based on Alignment of L/ODC Amino Acid Sequences in NCBI database, and were used to obtain the inner fragment of HsLDC cDNA sequence. 5′- and 3′-rapid amplification of cDNA ends were conducted by using 5′- and 3′-RACE Kit (Invitrogen). Primers used in this study were listed in Supplemental Table S1.

4.4. Sequence analysis

Basic Local Alignment Searches were performed with NCBI's BLAST (http://www.ncbi.nlm.nih.gov/). Multiple protein sequences alignment was performed on program Bioedit and the protein maximum likelihood tree was constructed using the program MEGA6.

4.5. Over-expression and purification of HsLDC

A culture of *E. coli* BL21(DE3) cells harboring the HsLDC/pET28a construct were grown in the LB medium containing 50 μg mL^{-1} of

Please cite this article in press as: Xu, B., et al., Identification and characterization of L-lysine decarboxylase from *Huperzia serrata* and its role in the metabolic pathway of lycopodium alkaloid, Phytochemistry (2017), http://dx.doi.org/10.1016/j.phytochem.2016.12.022

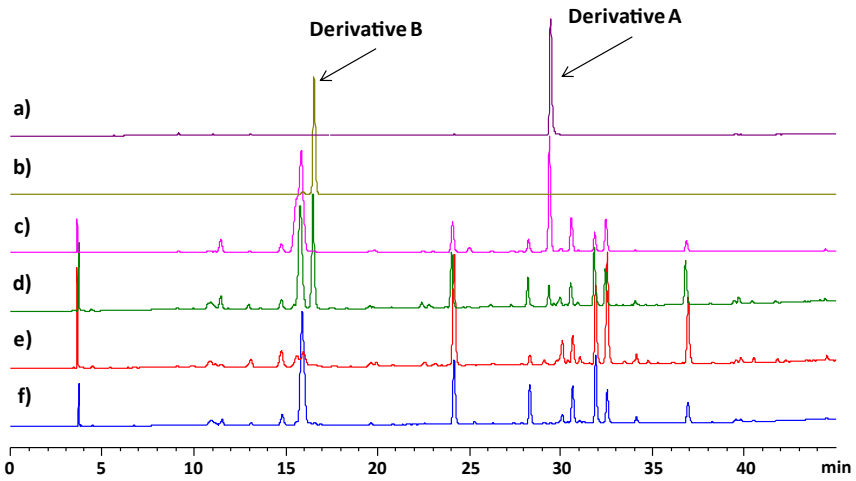

Fig. 7. HPLC analysis of 5-aminopentanal and cadaverine in transgenic tobacco leaves with the derivatization method. Trace a) **Derivative A** standard; trace b) **Derivative B** standard; trace c) Tobacco leaves transformed with HsLDC; trace d) Tobacco leaves transformed with HsLDC and HsCAO; trace e) Tobacco leaves transformed with blank vector; trace f) Wild-type tobacco leaves.

kanamycin at 37 °C with shaking (200 rpm) until the OD_{600} reached ~0.5. Protein expression was then induced by addition of isopropyl β-D-1-thiogalactopyranoside (IPTG) to a final concentration of 0.5 mM, and the cells were allowed to grow at 16 °C and 200 rpm for an additional 20 h. The cells were harvested by centrifugation at 4500 × g for 15 min. All purification steps were carried out at 4 °C using Ni-NTA resin and the HsLDC protein were washed and eluted by 20–250 mM imidazole in 25 mM Tris-HCl, 150 mM NaCl buffer (pH 8.0). The collected protein solution was dialyzed against 25 mM Tris-HCl, 150 mM NaCl buffer (pH 8.0) for three times. The protein solution was then flash-frozen in liquid nitrogen and stored at −80 °C until use. Protein concentration was determined by the Bradford assay using bovine serum albumin as the standard.

4.6. HsLDC kinetic study

The HsLDC activity assays were performed with the purified N-His_6-LDC incubated with NADH (1.75 mM), PEP (10.0 mM), PLP (0.80 mM), PEPC (PEP carboxylase) (2 units), MDH (malate dehydrogenase) (8.24 units), $MgCl_2$ (10 mM), and proper concentration of selected amino acid substrates in 200 μL reaction buffer (150 mM NaCl, 100 mM Tris-HCl, pH 7.5). The reaction was initiated by adding HsLDC (5.50 μM) at 37 °C and the reaction rate was measured with consumption of NADH at 340 nm by UV-Vis. Each assay was measured for 3 replicates.

4.7. Protein LC-MS/MS analysis

HsLDC (7.60 μM) was reconstituted by incubating with PLP (10 mM) on ice for 20 min. The solution was added with $NaBH_4$ (final concentration 158 mM) and incubated at 25 °C for 30 min. The reduced protein solution was loaded into SDS-PAGE for protein purification. The gel was stained with coomassie blue and the targeted protein was cut and digested by trypsin followed by analyzed with Thermo Scientific Q Exactive LC-MS/MS.

4.8. Plasmid construction and plant transformation

The full-length ORF of HsLDC or HsCAO was transferred to the Gateway Donor vector pDONOR207 (Invitrogen) to provide pDONOR207::HsLDC or HsCAO and subsequently to generate binary vector pEAQ-HT-DEST1::HsLDC or HsCAO by using the LR reaction (Life Technologies). pEAQ-HT-DEST1::HsLDC or HsCAO constructs were transformed into *Agrobacterium tumefaciens* strain GV3101 using the freeze-thaw method (Sainsbury et al., 2009).

Transformants were grown on LB plates containing 50 μg mL^{-1} kanamycin and 20 μg mL^{-1} rifampicin at 28 °C. One single colony of agrobacterium was inoculated in LB media (5.0 mL) contained the same antibiotics and grown overnight at 28 °C with shaking at 170 rpm. 1.0 mL of the overnight culture was used to inoculate 50 mL of LB media (with same antibiotics) and grew until OD_{600} reached 0.6. The bacteria were precipitated (5,000 g for 15 min) and the pellet was re-suspended in MES buffer (10 mM MES, 10 mM $MgCl_2$, pH 5.8) with 100 μM AS (acetosyringone), by adjusting OD_{600} to 0.4 for each strain. The suspensions were left on the bench (room temperature) for 30 min then were infiltrated on the abaxial surfaces of the leaves with 1.0 mL syringe. Plants were put back and grown under a 16 h light cycle after infiltration. Leaves were harvested after 2 days' post-infiltration, and flash frozen then stored at −80 °C. Biological replicates consisted of several leaves all from different tobacco plants. Leaves expressing GUS as a blank vector control. Meanwhile, wild type controls were set.

4.9. Derivatization and HPLC analysis

The Tobacco leaves sample preparation and derivatization procedure was referred to benzoylation reaction (Pinto et al., 2014) with some modifications. Tobacco leaves were lyophilized and 0.10 g lyophilized samples were steeped in 2.5 mL of 5% (v/v) cold $HClO_4$ and incubated at 4 °C for 2 h then ultrasonicated for 10 min. The supernatant was collected into a new 2.0 mL Eppendorf tube and centrifugated at 13 000 g for 5 min then the final supernatant (1.0 mL) was collected into another 10 mL Eppendorf tube with adding 1.0 mL of 5% (v/v) cold $HClO_4$. Specified concentration of standard cadaverine were dissolved in 2.0 mL of 5% (v/v) cold $HClO_4$. Borate buffer (0.5 M, pH 10.0) and NaOH (8.0 M) were used to adjust pH to 10. Then, 680 μL of 3,5-dinitrobenzoyl chloride (56 mM in acetonitrile) was added to the previous solution, which was subjected to overtax. Afterward, the mixture was ultrasonicated for 20 min at room temperature. NaCl (0.50 g) and CCl_4 (205 μL) were added into the solutions to extract the amine derivatives. The organic phase was collected and dried over Na_2SO_4 then re-dissolved in acetonitrile (0.10 mL) for HPLC analysis.

HPLC method: Two Columns, Column-1 (Luna 5u C18 (2) 100A

Please cite this article in press as: Xu, B., et al., Identification and characterization of L-lysine decarboxylase from *Huperzia serrata* and its role in the metabolic pathway of lycopodium alkaloid, Phytochemistry (2017), http://dx.doi.org/10.1016/j.phytochem.2016.12.022

Phenomenex column (250 × 4.6 mm)) and Column-2 (Synergi Fusion RP 4u 80A Phenomenex column (250 × 4.6 mm)) were used. The column temperature was set at 35 °C, and the chromatographic separation was carried out by gradient elution with two solvent mixtures at the flow rate of 1.0 mL min^{-1}. For Fig. 5B and Supplemental Fig. S14, Cloumn-1, Solvent A (10 mM aqueous sodium formate/formic acid buffer at pH 3.0) and solvent B (acetonitrile) were used. The linear gradient program was performed as follow: 0–10 min, 5–40% B; 10–30 min, 40–80% B; 30–35 min, 80–95% B; 35–40 min, 95% B; and 40–50 min, column rinse and re-equilibration. For Fig. 5D, Cloumn-2, Solvent A and solvent B were used. The linear gradient program was as above. For Fig. 7, Cloumn-1, Solvent A and solvent B were used. The linear gradient program was performed as follow: 0–10 min, 5–30% B; 10–20 min, 30% B; 20–35 min, 30–80% B; 35–40 min, 80–95%; 40–45 min, 95% B; and 45–55 min, column rinse and re-equilibration. Diode array detection was carried out at the wavelength of 260 nm.

Acknowledgments

This work was financially supported by the Science and Technology Commission of Shanghai Municipality (Grant 15JC1400402), CAS-JIC Centre of Excellence in Plant and Microbial Sciences (CEPAMS) funding, the “Thousand Talents Program” young investigator award, and the National Natural Science Foundation of China (Grant 21572243). Authors thank Dr. Yining Liu and Dr. Yuanhong Shan in the Core Facility Centre of the Institute of Plant Physiology and Ecology for mass spectrometry assistance. The authors also thank Prof. Dr. George P. Lomonossoff (John Innes Centre (JIC), UK) for providing the pEAQ vector.

Appendix A. Supplementary data

Supplementary data related to this article can be found at http://dx.doi.org/10.1016/j.phytochem.2016.12.022.

References

Ayer, W.A., Trifonov, L.S., . Lycopodium alkaloids. In: Cordell GA, Brossi A (eds) The Alkaloids: Chemistry and Pharmacology. Academic Press, San Diego, 45,233–266, Chapter 3.

Bai, F., Xu, Y.C., Chen, J., Liu, Q.F., Gu, J.F., Wang, X.C., Ma, J.P., Li, H.L., Onuchic, J.N., Jiang, H.L., 2013. Free energy landscape for the binding process of Huperzine A to acetylcholinesterase. Proc. Natl. Acad. Sci. U. S. A. 110, 4273–4278.

Bödeker, K., 1881. Lycopodin, das erste Alkaloïd der Gefässkryptogamen. Justus Liebigs Ann. Chem. 208, 363–367.

Brown, S., Clastre, M., Courdavault, V., O'Connor, S.E., 2015. De novo production of the plant-derived alkaloid strictosidine in yeast. Proc. Natl. Acad. Sci. U. S. A. 112, 3205–3210.

Bunsupa, S., Katayama, K., Ikeura, E., Oikawa, A., Toyooka, K., Saito, K., Yamazaki, M., 2012. Lysine decarboxylase catalyzes the first step of quinolizidine alkaloid biosynthesis and coevolved with alkaloid production in leguminosae. Plant Cell 24, 1202–1216.

Bunsupa, S., Hanada, K., Maruyama, A., Aoyagi, K., Komatsu, K., Ueno, H., Yamashita, M., Sasaki, R., Oikawa, A., Saito, K., Yamazaki, M., 2016. Molecular evolution and functional characterization of a bifunctional decarboxylase involved in lycopodium alkaloid biosynthesis. Plant Physiol. 171, 2432–2444.

Coleman, C.S., Stanley, B.A., Pegg, A.E., 1993. Effect of mutations at active site residues on the activity of ornithine decarboxylase and its inhibition by active site-directed irreversible inhibitors. J. Biol. Chem. 268, 24572–24579.

Facchini, P.J., De Luca, V., 2008. Opium poppy and Madagascar periwinkle: model non-model systems to investigate alkaloid biosynthesis in plants. Plant J. 54, 763–784.

Facchini, P.J., Huber-Allanach, K.L., Tari, L.W., 2000. Plant aromatic L-amino acid decarboxylases: evolution, biochemistry, regulation, and metabolic engineering applications. Phytochem 54, 121–138.

Fossati, E., Narcross, L., Ekins, A., Falgueyret, J.-P., Martin, V.J., 2015. Synthesis of morphinan alkaloids in Saccharomyces cerevisiae. PLoS One 10, e0124459.

Häkkinen, S.T., Tilleman, S., Swiatek, A., deSutter, V., Rischer, H., VanHoutte, I., van Onckelen, H., Hilson, P., Inze, D., Oksman-Caldentey, K.M., Goossens, A., 2007. Functional characterization of genes involved in pyridine alkaloid biosynthesis in tobacco. Phytochem 68, 2773–2785.

Hemscheidt, T., Spenser, I.D., 1993. Biosynthesis of lycopodine: incorporation of acetate via an intermediate with C2v symmetry. J. Am. Chem. Soc. 115, 3020–3021.

Hsiao, Y.H.E., Bahn, J.H., Lin, X., Chan, T.M., Wang, R., Xiao, X., 2016. Alternative splicing modulated by genetic variants demonstrates accelerated evolution regulated by highly conserved proteins. Genome Res. Gr 193359.

Ishii, S., Mizuguchi, H., Nishino, J., Hayashi, H., Kagamiyama, H., 1996. Functionally important residues of aromatic L-amino acid decarboxylase probed by sequence alignment and site-directed mutagenesis. J. Biol. Chem. 120, 369–376.

Kitajima, M., Takayama, H., 2012. Lycopodium alkaloids: isolation and asymmetric synthesis. Top. Curr. Chem. 309, 1–32.

Liu, J.S., Yu, C.M., Zhou, Y.Z., Han, Y.Y., Wu, F.W., Qi, B.F., Zhu, Y.L., 1986a. Study on the chemistry of huperzine a and huperzine B. Acta Chimica Sinica (Zhongguo yao li xue bao) 44, 1035–1040.

Liu, J.S., Zhu, Y.L., Yu, C.M., Zhou, Y.Z., Han, Y.Y., Wu, F.W., Qi, B.F., 1986b. The structures of huperzine A and B, two new alkaloids exhibiting marked anticholinesterase activity. Can. J. Chem. 64, 837–839.

Luo, H.M., Li, Y., Sun, C., Wu, Q.O., Song, J.Y., Sun, Y.Z., Steinmetz, A., Chen, S.L., 2010. Comparison of 454-ESTs from *Huperzia serrata* and *Phlegmariurus carinatus* reveals putative genes involved in lycopodium alkaloid biosynthesis and developmental regulation. BMC Plant Biol. 10, 209.

Ma, X.Q., Gang, D.R., 2004. The Lycopodium alkaloids. Nat. Prod. Rep. 21, 752–772.

Ma, X.Q., Tan, C.H., Zhu, D.Y., Gang, D.R., 2006. A survey of potential Huperzine A natural resources in China: the Huperziaceae. J. Ethnopharmacol. 104, 54–67.

Møldrup, M.E., Geu-Flores, F., de Vos, M., Olsen, C.E., Sun, J., Jander, G., Halkier, B.A., 2012. Engineering of benzylglucosinolate in tobacco provides proof-of-concept for dead-end trap crops genetically modified to attract Plutella xylostella (diamondback moth). Plant Biotech. J. 10, 435–442.

Nishino, J., Hayashi, H., Ishii, S., Kagamiyama, H., 1997. An anomalous side reaction of the Lys303 mutant aromatic L-amino acid decarboxylase unravels the role of the residue in catalysis. J. Biol. Chem. 121, 604–611.

Osterman, A., Grishin, N.V., Kinch, L.N., Phillips, M.A., 1994. Formation of functional cross-species heterodimers of ornithine decarboxylase. Biochemistry 33, 13662–13667.

Osterman, A.L., Brooks, H.B., Jackson, L., Abbott, J.J., Phillips, M.A., 1999. Lysine-69 plays a key role in catalysis by ornithine decarboxylase through acceleration of the Schiff base formation, decarboxylation, and product release steps. Biochemistry 38, 11814–11826.

Phan, A.P., Ngo, T.T., Lenhoff, H.M., 1982. Spectrophotometric assay for lysine decarboxylase. Anal. Biochem. 120, 93–197.

Pinto, E., Melo, A., Ferreira, I.M., 2014. Sensitive quantitation of polyamines in plant foods by ultrasound-assisted benzoylation and dispersive liquid-liquid microextraction with the aid of experimental designs. J. Agric. Food. Chem. 62, 4276–4284.

Sainsbury, F., Thuenemann, E.C., Lomonossoff, G.P., 2009. pEAQ: versatile expression vectors for easy and quick transient expression of heterologous proteins in plants. Plant Biotech. J. 7, 682–693.

Smanski, M.J., Zhou, H., Claesen, J., Shen, B., Fischbach, M.A., Voigt, C.A., 2016. Synthetic biology to access and expand nature's chemical diversity. Nat. Rev. Microbiol. 14, 135–149.

Sun, J., Morita, H., Chen, G., Noguchi, H., Abe, I., 2012. Molecular cloning and characterization of copper amine oxidase from *Huperzia serrata*. Bioorg. Med. Chem. Lett. 22, 5784–5790.

Tang, X.C., De Sarno, P., Sugaya, K., Giacobini, E., 1989. Effect of huperzine A, a new cholinesterase inhibitor, on the central cholinergic system of the rat. J. Neurosci. Res. 24, 276–285.

Tang, X.C., Han, Y.F., Chen, X.P., Zhu, X.D., 1986. Effects of huperzine A on learning and the retrieval process of discrimination performance in rats. Acta pharmacologica Sinica (Zhongguo yao li xue bao) 7, 507–511.

Thodey, K., Galanie, S., Smolke, C.D., 2014. A microbial biomanufacturing platform for natural and semisynthetic opioids. Nat. Chem. Biol. 10, 837–844.

Zhang, X.C., Wei, R., Liu, H.M., He, L.J., Wang, L., Zhang, G.M., 2013. Phylogeny and classification of the extant lycophytes and ferns from China. Chin. Bull. Bot. 48, 119–137.

Ziegler, J., Facchini, P.J., 2008. Alkaloid biosynthesis: metabolism and trafficking. Annu. Rev. Plant Biol. 59, 735–769.

Please cite this article in press as: Xu, B., et al., Identification and characterization of L-lysine decarboxylase from *Huperzia serrata* and its role in the metabolic pathway of lycopodium alkaloid, Phytochemistry (2017), http://dx.doi.org/10.1016/j.phytochem.2016.12.022